

# A TerraSAR-X Experiment for Validation of Nadir Echo Suppression through Waveform Encoding and Dual-Focus Post-Processing

Se-Yeon Jeon, Thomas Kraus, Ulrich Steinbrecher, Michelangelo Villano, and Gerhard Krieger  
German Aerospace Center (DLR), Microwaves and Radar Institute, Wessling, Germany

## Abstract

Synthetic aperture radar (SAR) is a powerful remote sensing technique providing high-resolution images of the Earth's surface. The pulsed operation of SAR may cause nadir echoes in SAR images, which significantly affect the image quality and are therefore avoided through proper selection of the pulse repetition frequency (PRF). As an alternative, a novel concept for nadir echo suppression using waveform encoding and dual-focus post-processing can be exploited to alleviate the constraint on the PRF selection. This work validates this technique through a TerraSAR-X experiment. An acquisition has been performed with up- and down-chirp variation on a scenario, where the nadir echo is expected to appear, and suppression of the nadir echo by means of the proposed post-processing approach has been demonstrated.

## 1 Introduction

Synthetic aperture radar (SAR) is a technique that provides high resolution images for remote sensing regardless of sunlight and weather conditions [1].

The pulsed operation of SAR leads to the simultaneous return of the echoes reflected from the point with shortest range from the radar, i.e., the nadir, and the echoes from the desired scene. The nadir echo may significantly affect the SAR image quality due to its strong intensity, because of the shorter distance and the specular reflection process. The nadir echo is typically seen as a bright stripe in the SAR image as shown in **Figure 1**.

In the design of conventional spaceborne SAR systems the nadir interference in SAR images is avoided by proper selection of the pulse repetition frequency (PRF). The timing diagram of a SAR system for PRF selection is shown in **Figure 2**. The blue areas represent the blind ground ranges, which cannot be imaged due to the transmit interference, while the green areas represent ground ranges, where nadir interference is present in the imaged scene. Some possible imaged swaths are shown with red lines in **Figure 2** and the corresponding PRF are selected to avoid both transmit and nadir interferences [2].

The constraint on the PRF selection, additionally imposed by the nadir echoes, limits the SAR system performance in terms of achievable swath widths and azimuth ambiguity levels. Therefore, nadir echo suppression can alleviate the constraint on the PRF selection so that given requirements can be achieved without increasing the system complexity or the antenna height.

To relieve the constraint on the PRF selection imposed by the nadir interference, an innovative concept using waveform-encoding and dual-focus post-processing for nadir echo suppression was proposed in [3]. This method exploits pulse-to-pulse waveform variation on transmit, and different matched filters in post-processing for nadir echo removal. This concept also leads to range ambiguity

smearing and can be to some extent exploited for suppression of strong range ambiguities [4], [5].

This work presents a validation of this technique through a TerraSAR-X experiment, where the nadir echo appearing in the acquired SAR image is suppressed through dual-focus post-processing.

## 2 The Waveform-Encoded SAR Concept

The nadir echo can be smeared within pulse or range compression, if different “orthogonal” waveforms are used for the two transmitted pulses corresponding to the useful signal and the nadir echo, such as an up- and down-chirp alternation [6].

The waveform variation scheme and the superposition of the resulting nadir echo and useful signal are shown in **Figure 3**. If smeared, the nadir echo is less visible, however, it still appears as a background noise, which may interfere with retrieving information from SAR images. By applying a further technique allowed by the waveform-encoding, i.e., the dual-focus post-processing, the nadir echo is not only smeared but can be removed [3].

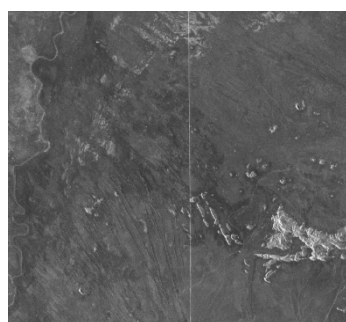


**Figure 1** TerraSAR-X image over Australia as an example of nadir echo in a SAR image, where the horizontal and vertical axes represent slant range and azimuth, respectively. The nadir echo, a bright vertical line, appears in the middle of the image.

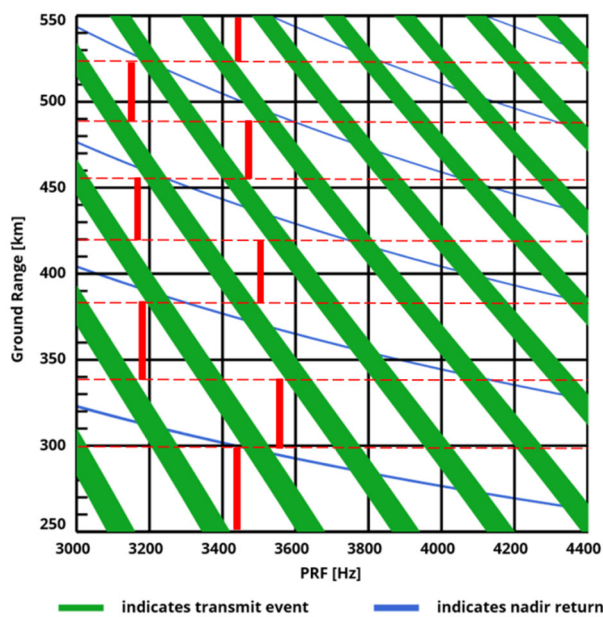


**Figure 2** Timing diagram for PRF selection of conventional SAR. The green and blue areas are transmit and nadir interferences, respectively, while the red lines indicate possible swaths that avoid transmit and nadir interferences.

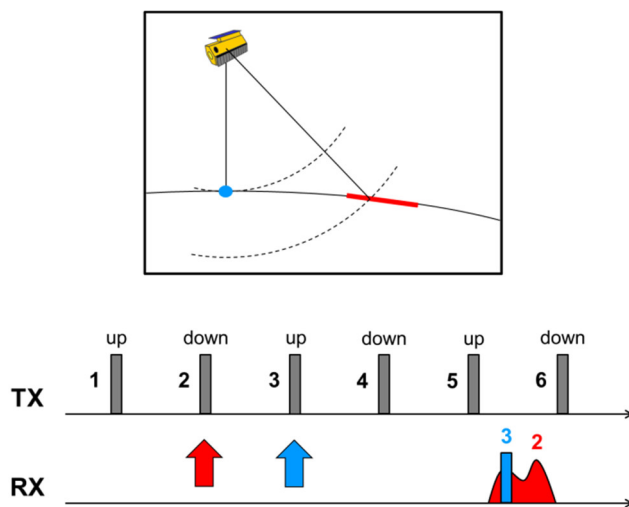


**Figure 3** Waveform variation scheme, and superposition of nadir echo (blue) and useful signal (red) in the received signal.

The processing steps of a dual-focus post-processing for waveform-encoded SAR system to suppress the nadir echoes are shown as a block diagram in **Figure 4**. By applying a filter matched to the nadir echo on the raw SAR data, the nadir echoes are focused on a certain range while the useful signal is smeared over the ranges. The focused nadir echo can be removed without significant degradation of the useful signal. The removal of the focused nadir echo is performed by simply replacing the pixel values into zeros. The location of nadir echo can be either determined from the PRF, the orbit information, and a digital

elevation model (DEM) of the scene, or by application of an adaptive threshold. The data which nadir echoes have been removed are inverse focused back into raw data and then focused with a filter matched to the useful signal.

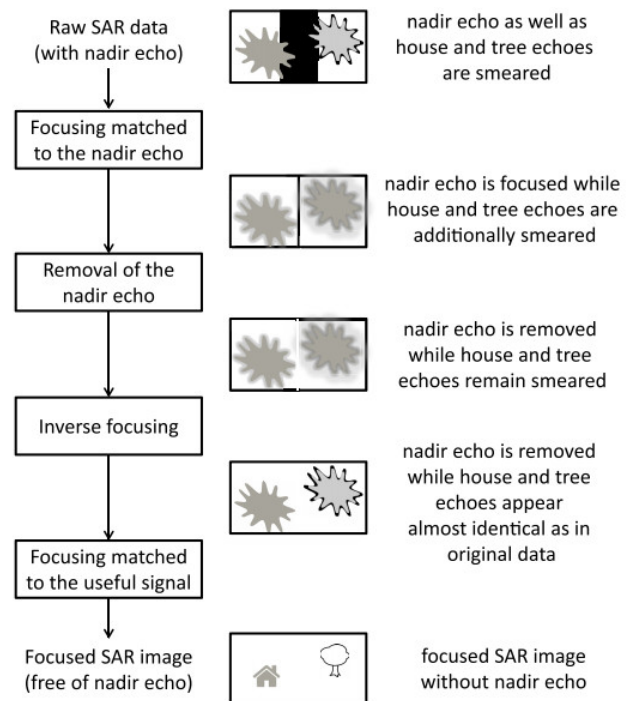


**Figure 4** Block diagram of dual-focus post-processing steps of waveform-encoded SAR for nadir echo suppression.

### 3 TerraSAR-X Experiment

#### 3.1 Experimental Setup

An experiment was executed to validate the proposed technique using TerraSAR-X. The scene was selected considering a scenario, where the nadir echo is expected to appear in the image, in order to show that nadir echoes can be suppressed through waveform-encoding and dual-focus post-processing. The scene includes a calm water surface from which a strong nadir echo return is expected and an urban area with strong scatterers in the imaged swath, as illustrated in Figure 5. TerraSAR-X data were acquired over an area that satisfies this property, namely near Tianjin, China, as of July 2019. Several acquisitions were needed to obtain data with visible nadir echoes, due to the varying wind conditions that impact the water surface and its scattering characteristics. The detailed geometry of the SAR data acquisition is depicted in Figure 6. The red line indicates the imaged ground swath ranging from 207 km to 224 km, while the nadir echo is expected to appear at a ground range of about 214 km.

The system parameters of TerraSAR-X for the experiment are provided in **Table 1**. The waveform variation during the experiment was arranged as shown in **Figure 7**, i.e., three up chirps and a down chirp were alternated, to acquire an interleaved reference image with the same pa-

rameters, geometry, and scene as the waveform-encoded SAR image, in order to perform comparison analyses. The PRF of TerraSAR-X is therefore twice the PRF of each image to be processed.

**Figure 8** shows the reference SAR image of the scene using only up chirps as described in Figure 7.

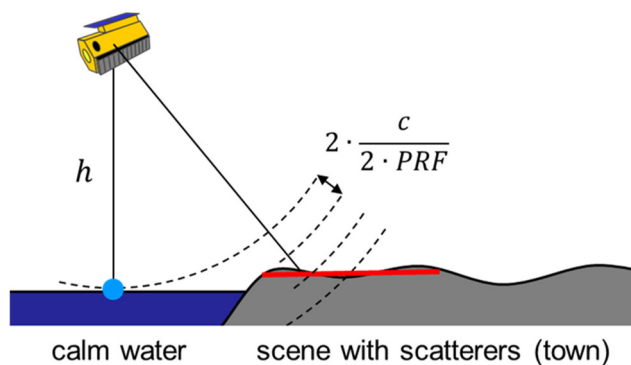


**Figure 5** Properties of the selected scene.

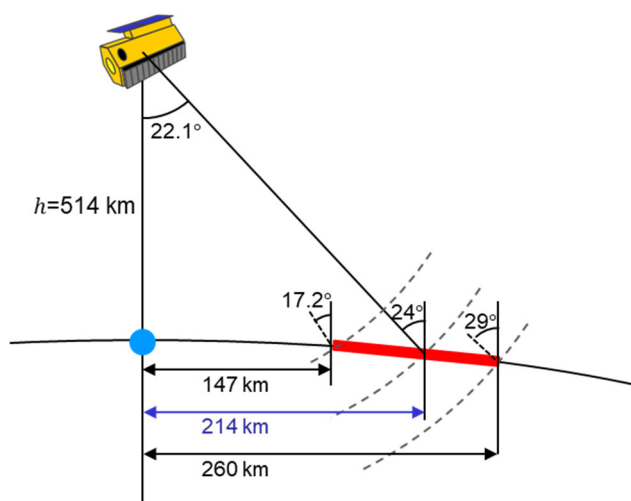


**Figure 6** Geometry of SAR image acquisition.

**Table 1** Experimental parameters.

Parameter	Value
Frequency	9.65 GHz
Orbit height	513 km
Chirp bandwidth	100 MHz
Chirp duration	15 $\mu$ s
PRF	6616 Hz
Incident angle	23.7° – 25.4°
Ground range of nadir echo	214 km

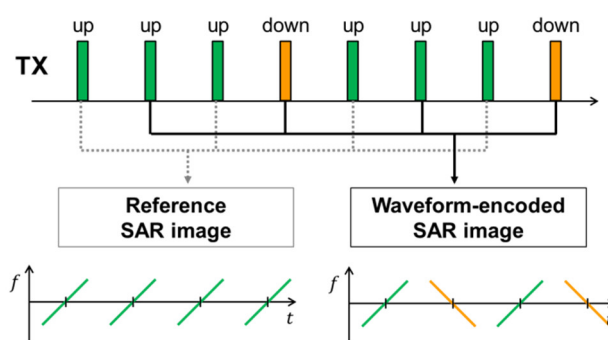


**Figure 7** Waveform variation scheme for the experimental validation with TerraSAR-X.

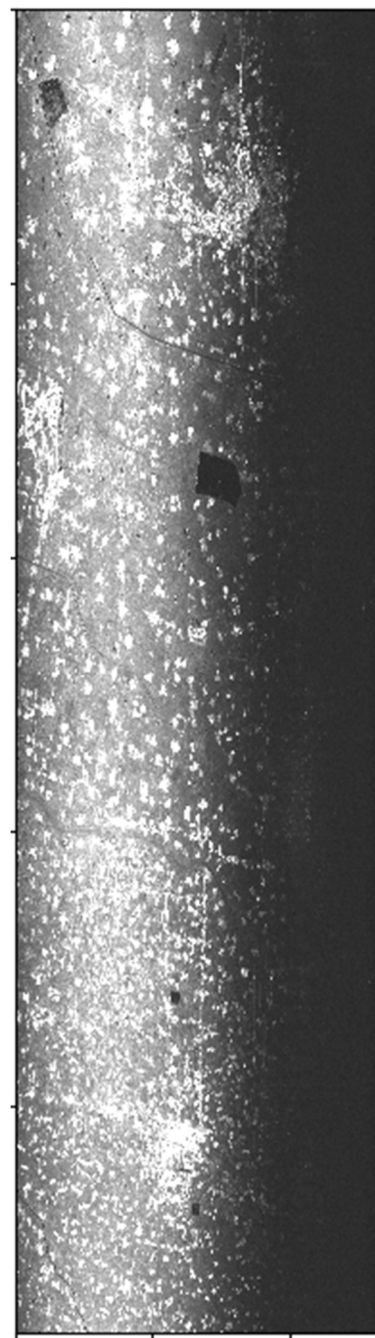


**Figure 8** Reference SAR image of the scene using conventional SAR. The horizontal and vertical axes represent slant range and azimuth, respectively.

### 3.2 Nadir Echo Suppression through Post-Processing

**Figure 9** (a) and (b) shows the range compressed data for the reference and the waveform encoded SAR data, respectively, obtained using a filter matched to the useful signal. The red boxes highlight the areas where the nadir echo is visible. While the nadir echo is visible as bright dashes in the reference case, in the waveform-encoded SAR case (if range compression is matched to the useful signal) the nadir echo is smeared in the range direction. Then the post-processing is introduced by applying a filter matched to the nadir echo to the waveform-encoded raw data, that allows highlighting the nadir echo, as shown in **Figure 9** (c) and blanking it in the range-compressed data.

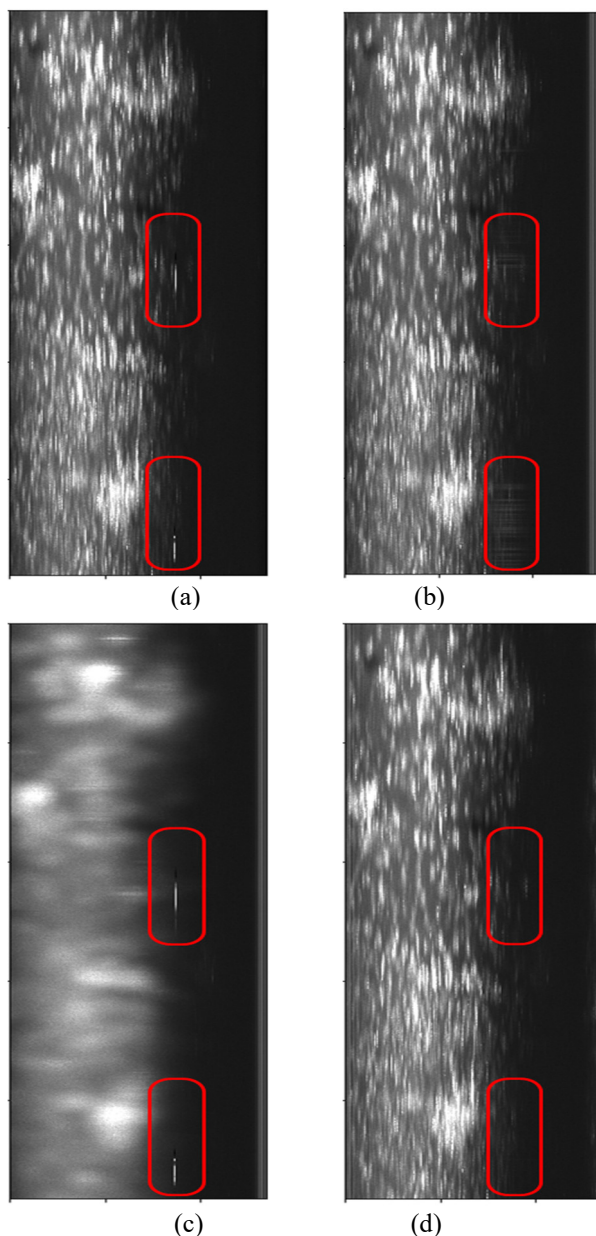


**Figure 9** Range-compressed data of (a) reference, (b) waveform-encoded SAR with filter matched to the useful signal, (c) waveform-encoded SAR with filter matched to the nadir echo, and (d) waveform-encoded SAR after dual-focus post-processing. The horizontal and vertical axes represent slant range and azimuth, respectively.

The range-compressed data, where the nadir echo has been removed, is decompressed back to the raw data and then compressed again with a filter matched to the useful signal. The final post-processed range-compressed data are shown in **Figure 9** (d). The dual-focus post-processing is not only smearing but significantly suppressing the nadir echo. Seven range samples were blanked for each azimuth. Zooms of the range-compressed data, where the nadir echo is mostly visible/expected to be located, are shown in **Figure 10**.

### 3.3 Performance Analysis

In order to understand how effective the nadir echo suppression is, some profiles obtained by averaging the range-compressed data over azimuth are shown in **Figure 11**, which refer to the zoomed area in **Figure 10**. Differences of the intensities between the averaged range profiles of waveform-encoded SAR (without and with post-processing) and the reference are also displayed. From the profiles it is apparent that the post-processing completely suppresses the nadir echo, characterized by an intensity about 3-4 dB higher than the background data. Further investigations will be conducted to understand whether it is preferable to blank the nadir echo in range-compressed or focused data.

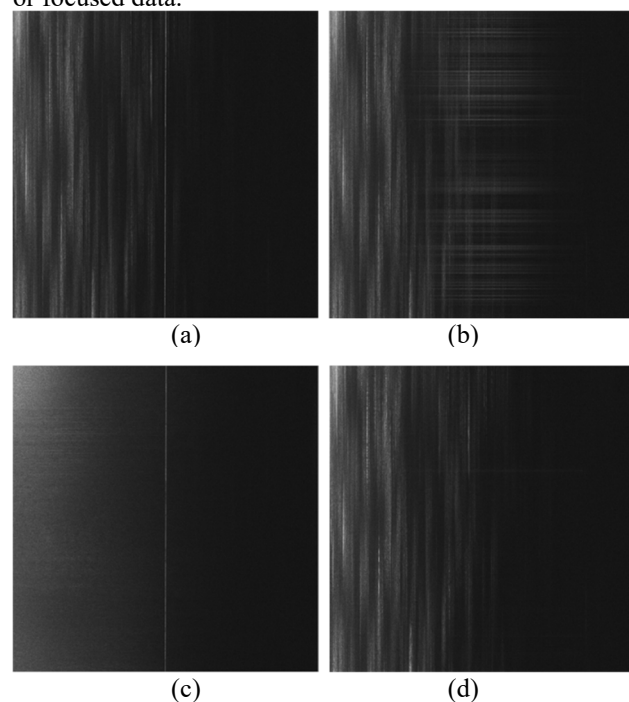


**Figure 10** Zoomed and nadir echo centered range-compressed data of (a) reference, (b) waveform-encoded SAR with filter matched to the useful signal, (c) waveform-encoded SAR with filter matched to the nadir echo, and (d) waveform-encoded SAR after dual-focus post-processing. The horizontal and vertical axes represent slant range and azimuth, respectively.

## 4 Conclusion

The novel SAR technique using waveform-encoding and dual-focus post-processing for nadir echo suppression has been validated with a TerraSAR-X experiment. A prelim-



inary analysis of the TerraSAR-X data shows that the proposed technique can effectively suppress (and not only smear) the nadir echo.

[6]

J. Mittermayer and J. M. Martinez, “Analysis of range ambiguity suppression in SAR by up and down chirp modulation for point and distributed targets,” in *in IGARSS 2003. 2003 IEEE International Geoscience and Remote Sensing Symposium. Proceedings 2003*, vol. 6, pp. 4077–4079 vol.6.

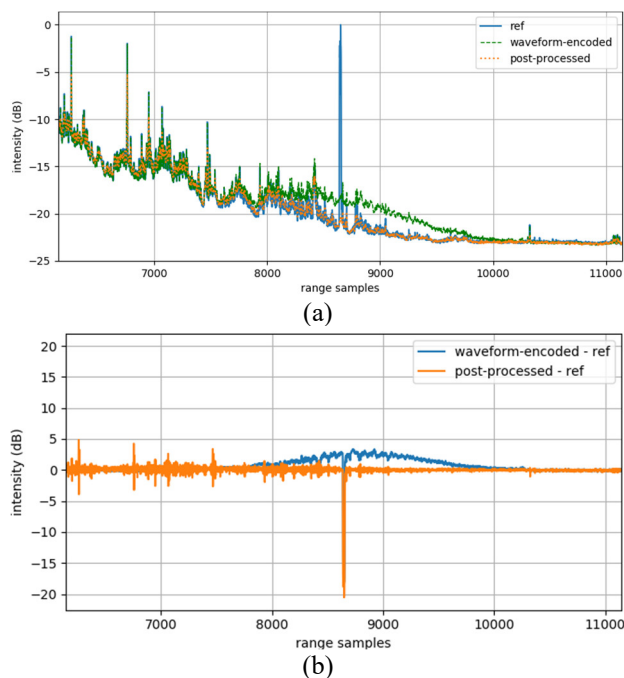


**Figure 11** (a) Intensity averaged over the azimuth direction (in dB). (b) Differences of the intensities of the averaged range profiles of the waveform-encoded SAR (without and with post-processing) and the reference.

## 5 Literature

- [1] A. Moreira et al., “A tutorial on synthetic aperture radar,” *IEEE Geosci. Remote Sens. Mag.*, pp. vol. 1, no. 1, pp. 6–43, Jan. 2013.
- [2] J. C. Curlander and R. N. McDonough, *Synthetic Aperture Radar: Systems and Signal Processing*, New York, NY, USA: Wiley, 1991.
- [3] M. Villano, G. Krieger, and A. Moreira, “Nadir Echo Removal in Synthetic Aperture Radar via Waveform Diversity and Dual-Focus Postprocessing,” *IEEE Geosci. Remote Sens. Lett.*, vol. 15, no. 5, p. 719–723, May 2018.
- [4] M. Villano, G. Krieger, and A. Moreira, “Waveform-Encoded SAR: A Novel Concept for Nadir Echo and Range Ambiguity Suppression,” in *EUSAR 2018; 12th European Conference on Synthetic Aperture Radar*, Aachen, Germany, 2018, pp. 1–6.
- [5] L. Dell’Amore, M. Villano, and G. Krieger, “Assessment of Image Quality of Waveform-Encoded Synthetic Aperture Radar Using Real Satellite Data,” in *2019 20th International Radar Symposium (IRS)*, 2019, pp. 1–10.